SEPTEMBER 2022

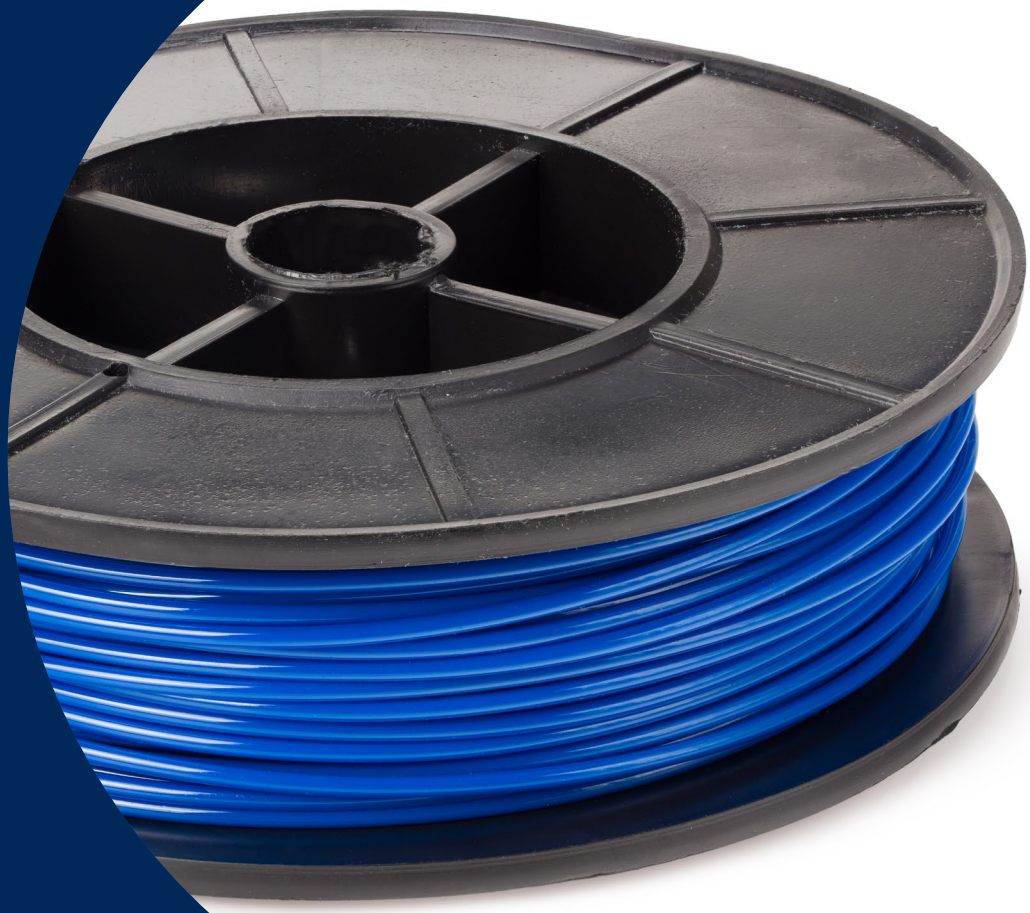

FINAL REPORT

Dosimetric and Toxicological Analysis of 3D Printer Emitted Particles

Provided by Georgia State University, School of Public Health
Principal Investigator, Dr. Christa Wright

UL Research Institutes | Chemical Insights

Table of Contents

List of Figures

List of Tables

Abstract

Three-dimensional printing (3DP) is an exciting innovation that has transformed research, manufacturing, and student experience particularly in STEM curricula throughout secondary and post-secondary education. As with so many new technologies, there are unintended safety and health considerations that must be managed. Fused filament fabrication is a popular 3DP method that involves heating, cooling, and manipulating thermoplastics that can result in airborne emissions of numerous chemicals and particulate matter (PM). This report provides scientific insights on the potential toxicological properties of inhaled particles emitted from FFF 3D printers during operation.

Aerosol measurement tools were used to study the particle emissions from two of the most common 3DP filaments, acrylonitrile butadiene styrene (ABS) and polylactic acid (PLA). Using Multiple Path Particle Dosimetry (MPPD) software, the level of particle deposition based on specific lung and breathing characteristics was determined. Human airway epithelial cells were exposed to 3DP particles and various cellular bioassays and metabolomic profiling were employed to assess the potential for cellular injury, inflammation, and oxidative stress which can lead to DNA damage within cells.

SUMMARY FINDINGS INCLUDE:

- 3DP emissions, even at low levels, may contribute to cellular injury, inflammation, and oxidative damage of important biomolecules including DNA and phospholipids that serve critical roles in living cells.
- Exposure to 3DP emissions using both PLA and ABS filaments was associated with a decline in airway cell viability, oxidative stress, an increase in DNA damage, and high levels of metabolites (products of metabolism) that are associated with cellular injury and inflammation.
- Maintaining a safe distance from 3DP during printer operation should be discussed as part of recommended safety guidelines along with ventilation and filtration mitigation strategies.

1.0 Report Purpose

This research was performed to assess the toxicological properties of emitted particulate matter (PM) from 3D printers and to determine the toxicity of popular filaments using primary small airway epithelial cells and physiologically relevant PM doses.

The research was led by Dr. Christa Wright previously of Georgia State University (GSU) with the support of graduate student Jennifer Jeon. Research Staff of Chemical Insights Research Institute (CIRI) of UL Research Institutes provided support in the collection of air samples from various school environments during the operation of 3D printers (3DPs). The following report was provided by the principal investigator.

2.0 Rationale and Aims

Rationale: Three-dimensional (3D) printing consists of heating, cooling, and manipulating thermoplastics, which may cause the emission of hazardous chemical compounds. Given the popularity of 3D printers in STEM curriculum within secondary and post-secondary educational settings, it is essential to determine the following questions: (1) Which filaments pose the greatest health risk or hazard? (2) At what conditions are inhalation risks greater? (3) What are the toxicological properties of potentially inhaled 3D printer emissions at doses based on actual PM aerosol properties?

THE FOLLOWING AIMS WERE EVALUATED:

- **Aim 1: Evaluate the potential PM mass inhaled and deposited within the lungs of adolescent and adult 3D printer users.** Within this aim, we evaluated the level of particle concentrations and size distributions for each feedstock material across a three-hour printing duration. The aerosol data were inputted into a computational software called the Multiple Path Particle Dosimetry (MPPD). The MPPD model determined the level of potential particle deposition based on the specific lung and breathing characteristics. The deposition mass values then served as starting dose ranges in the in vitro exposures and toxicological testing strategy.
- **Aim 2: Determine and compare the toxicological profiles of emitted PM generated by each filament based on inhalation dosimetric considerations.** Using small airway epithelial cells, we examined the cellular responses to 3D printer PM exposures derived from each feedstock material at a local university and high school. We then utilized cell-based assays including reactive oxygen species detection and metabolic activity assays to assess the bioactivity of the 3D printer PM. Cytokine and chemokine levels were also measured in cellular supernatants using Eve Technologies ELISA array technology. Finally, metabolomic profiles of each 3D printer PM were assessed to determine the unique metabolite signatures generated by each filament.

3.0 Experimental Methods

3.1 SAMPLING SITES

3D printer emitted PM samples were collected from two locations: (1) university; (2) high school. All safety procedures were followed during sampling and in vitro toxicological evaluations according to GSU Biosafety guidelines protocol # BE21021.

3.2 3D PRINTER PM MONITORING AND SAMPLING SITES AND PROTOCOL

3D printer PM emissions were measured across a three-hour printing duration. Aerosol size distributions were assessed using a scanning mobility particle sizer (SMPS) in tandem with an aerodynamic particle sizer (APS) to detect a broad particle size range (2.5 nm to 20 microns). Total aerosol size fractions were sampled and collected onto polycarbonate filters. Pre and post filter weights were obtained accordingly. The sampling strategy shown in **Table 1** as provided by CIRI Research Scientist Dr. Aika Davis was implemented.

Table 1: 3D Printer Sampling Strategy and Site Assessment

Activity	Time
Site survey	Day 1
3D printer installation and instructions	Day 1
Questionnaire about potential usage	Day 1
Air quality monitoring setup	Day 1
Air quality background	Day 2 morning
Air monitoring during a 3 hour 3D print with Polylactic Acid (PLA)	Day 2: 3 hours
Cleanup and monitoring setup for test with Acrylonitrile Butadiene Styrene (ABS)	Day 2
Air quality background	Day 3 morning
Air monitoring during a 3 hour 3D print with ABS	Day 3: 3 hours
Pack up	Day 3
Data analysis	Subsequent weeks
Report back on assessment, suggest and implement further safety practices, if applicable, followed by additional testing.	Another day

3.3 PM EXTRACTION

A subset of 3D emitted particles/Teflon filters were extracted using a solvent-based (75% methanol) method coupled with sonication. 3D printer emitted particle extractions were vacufuged to remove the solvent extraction fluid. Vacufuged samples were refrigerated until toxicological analysis.

3.4 IN VITRO DOSIMETRIC CONSIDERATIONS

PM doses were determined by inputting aerosol data (geometric mean diameter, aerosol concentration) into the Multiple-Path Particle Dosimetry (MPPD) computational model as previously described. The parameters used by MPPD software to calculate deposition comprise four areas: (1) the type of airway morphometry was age-specific (14 years old) symmetric; (2) the particle properties included count median diameter (CMD) and geometric standard deviation (GSD), (3) the exposure was a constant exposure at measured PM concentration, and (4) the deposition and clearance of the particles. The exposure time was assumed to be 6 hours per day, 5 days per week for a school year of 36 weeks. The total deposited mass across the airways (Generations 1-21) was divided by the surface area of those regions, which provided the total deposited dose within the small airways. To convert the total deposited dose to an in vitro concentration, we multiplied the total deposited dose ($\mu g/cm^2$) by the surface area of one well within a 96 well plate (0.33 cm^2) then divided by the total exposure volume (0.1 ml).

3.5 CELL CULTURE AND EXPOSURE

Normal small airway epithelial cells (SAEC) were cultured in small airway basal media (SABM) (Lonza, Walkersville, MD) supplemented with bovine pituitary extract (BPE), hydrocortisone, human epidermal growth factor (hEGF), epinephrine, transferrin, insulin, retinoic acid, triiodothyronine, gentamicin, amphotericin-B (GA-1000). SAEC were incubated in a humidified atmosphere of 37ºC/5% CO_2 until 3DP PM exposure. For 3DP PM exposures, SAEC were subcultured into 96 well plates at a density of 10,000 cells/well and grown to 70-80% confluency for 5-7 days. 3D printer emitted particles collected during sampling were extracted and diluted into cell culture media and administered to submerged SAEC in 96 well plates in a volume of 100 µl.

3.6 TOXICOLOGICAL EVALUATION APPROACH

Toxicological assessments were performed for each collected PM filter sample that contained sufficient mass. Metabolic activity or cellular viability was assessed via the MTS assay, gamma-H2AX – a biomarker of double stranded DNA damage was performed using enzyme linked immunoassay (ELISA) and metabolic profiling on SAEC supernatants were performed at Purdue University. The following describes the methods utilized:

MTS Assay

Metabolic activity was measured using the CellTiter 96 Aqueous One Solution (MTS) (Promega) assay. Briefly, cells (10,000 cells/well) were seeded in 96 well plates (Corning Inc., New York, NY) and maintained until 70-80% confluency. Diluted 3DP extracts in cell culture media called SABM at 5 and 10 µg/ml concentrations were administered to the cells/well, then incubated for 24 hours. After exposure, control and exposed cells were washed twice with 1x phosphate buffered saline (PBS). SABM containing MTS reagent was added for 45 minutes and read at 490 nm using a microplate reader (Cytation 1, Biotek). Media and vehicle/blank controls were evaluated to ensure assay integrity.

Gamma-H2AX Evaluation

Gamma-H2AX ELISA assay (R&D Systems) was used to indirectly determine 3DP PM mediated double stranded DNA breaks. Following 24 hour 3DP exposures, SAEC were lyzed using a hypotonic solution and lysates were added to R&D Systems antibody coated wells for 3 hours. After incubation, H2AX detection antibody was added to the wells followed by addition of a goat anti-Mouse IgM HRP conjugate and a chemiluminescent HRP substrate, which produces relative light units (RLU) that directly correlate with the amount of gamma-H2AX in the sample. All manufacturer's instructions were followed.

Metabolomic Profiling

Following PM exposures, cell media/supernatants and pellets were collected. The Blyth and Dyer method, consisting of a methanol/water/chloroform extraction, were performed on samples (pellet and supernatant). HPLC-MS-MS (QTof) was used for global profiling to assess the water/methanol (metabolite) and the chloroform (lipid) fractions thus providing a thorough data set allowing for the identification of released and internally modified compounds. Separations were performed on an Agilent 1290 system. Metabolites were assayed using a Waters HSS T3 column and lipids were assayed using a Zorbax C18 column, both using a water and acetonitrile gradient. Mass analysis were obtained using an Agilent 6545 Q-tof mass spectrometer with mass data collected using Agilent MassHunter Acquisition software. MS/MS were performed in a data-dependent acquisition mode to aid in compound identification. Specific alterations in metabolites that indicate cellular injury including PGE-2 (inflammation), glutathione and oxidized phospholipids (oxidative stress), and the glucuronidation pathway (xenobiotic metabolism) were measured and assessed.

3.7 STATISTICAL ANALYSIS

For all cellular outcomes, descriptive statistics and histograms by exposure group and monitoring location were provided using GraphPad 6 Prism software and one-way ANOVA followed by a Bonferroni's post-hoc analysis. P-values less than or equal to 0.05 were denoted as significant (*). For metabolomics analysis, a fold change of 2 or higher along with p-value of less than or equal to 0.05 were deemed significant.

4.0 Results and Discussion

4.1 3DP AEROSOL CHARACTERIZATION AND IN VITRO DOSIMETRY

Aerosol characterization data collected by CIRI Research Scientist Dr. Qian Zhang and filter site descriptions are presented in **Table 2**. Additionally, the average inhaled dose and in vitro dose for the cellular analyses were determined from the aerosol concentration, count mean diameter (CMD), and geometric standard deviation (GSD) obtained from each site location.

The average aerosol concentration across all sites was 4.16 µg/m^3. The average count mean diameter or CMD was found to be 116.4 nm. The average potentially inhaled dose across all filaments and sampling locations for a teenager of 14 years old or a 21-year-old was 2.02 µg/cm^2. The average in vitro dose across all filaments and locations was 6.66 µg/ml with a range of 4.42 to 10.4 µg/ml. It should be noted that 10 µg/ml and 5 µg/ml were utilized as the administered high and low concentrations to cover the range of extrapolated in vitro doses described in **Table 2**. Preliminary dose response assessments showed concentrations below 5 µg/ml were not cytotoxic (data not shown).

Table 2: Aerosol Characterization, Inhaled Doses, and Calculated In Vitro Dose for 3DP Emissions

Filter Label	Print Scenario	Sample Location	CMD (nm)	GSD	Mass Concentration (µg/m^3)	Potentially Inhaled Dose (µg/cm^2)	In Vitro Dose (µg/ml)
F2	ABS	HS CTRL	122	1.79	3.34	2.03	6.69
F3	ABS	HS 3DP NEAR	87.4	1.94	4.33	1.46	4.81
F4	ABS	HS 3DP FAR	116	1.82	3.19	1.94	6.39
F6	PLA	HS CTRL	128	1.75	5.09	2.14	7.05
F7	PLA	HS 3DP NEAR	130	1.77	4.44	2.16	7.14
F8	PLA	HS 3DP FAR	126	1.78	4.86	2.10	6.92
F1	ABS	UNI SLAB NEAR	91.1	1.92	2.22	1.52	5.01
F5	ABS	UNI SLAB FAR	146	1.78	4.52	2.43	8.03
F9	ABS	UNI CTRL	112	1.92	4.24	1.87	6.16
F10	ABS	UNI OBS	189	1.53	7.15	3.15	10.4
F12	PLA	UNI LAB NEAR	163	2.75	1.48	0.62	2.04
F15	PLA	UNI CONF RM	37.2	1.72	0.88	1.34	4.42

Legend: HS=high school, UNI=university, 3DP=3D printer room, CTRL=control room without 3D printers, SLAB=small lab, OBS=outside biosafety cabinet, CONF RM=conference room

4.2 THE IMPACT OF FILAMENT AND SITE LOCATION ON CELLULAR VIABILITY OF SAEC

The MTS assay was employed to determine the metabolic capacity of SAEC after 3DP particle exposure. The level or percentage of metabolic capacity retained by the cells after 3DP particle exposure is a measure of cellular viability. Hence, untreated cells should possess 100% metabolic capacity or cellular viability whereas positive control treated cells may fall significantly below that of the untreated or negative control cells. SAEC cells exposed to 3DP filter samples will fall typically between the negative and positive control viability levels or percentages.

After 24 hours, the MTS assay was utilized to assess the biological activity and toxic potential of particles emitted during ABS and PLA filament usage. In each of the figures, the y-axis contains the percent control, which normalizes all sample data to the negative or untreated control (NC) cells by dividing the average optical density value of the 3DP exposure groups by the average of the NC optical density then multiplying by 100, thus providing the percent control. The x-axis contains the exposure groups and their respective site locations along with experimental controls including a positive control (PC) consisting of 0.1% hypotonic solution (Triton-X) and blank controls (BLK), which contains an empty or filter blank extracted solution that was subjected to the same extraction methods as the site filter samples.

Panel A of Figure 1 shows the metabolic activity or cellular viability of SAEC exposed to 3DP particles derived from ABS filament collected at the high school in July 2021. In comparison to the negative control or untreated cell group, 3DP ABS particles collected near the printer at the high dose (10 µg/ml) (F3-H) elicited a significant reduction (49.5%) in cellular viability. Likewise, 3DP ABS particles collected far from the printer for both low and high doses (F4-L,F4-H) contributed to a decline in cellular viability in comparison to untreated cells. Interestingly, particle samples obtained from control rooms adjacent to 3DP sampling rooms altered cellular viability slightly but not significantly by 18.2% and 15.4%, respectively, for low (F2-L) and high doses (F2-H). **Panel B** highlights modifications to SAEC cellular viability imposed by particles emitted during a 3 hour PLA print process. 3DP particles sampled near the printer at both the high and low doses were highly toxic leading to a 40.8% (F7-H) and 56% (F7-L) decline in cellular viability, respectively. Low doses of PLA (F8-L) elicited a significant reduction of cellular viability unlike the high dose. Like the control room of ABS, the samples collected at the same time in the adjacent classroom (F6-L,F6-H) during PLA printing also diminished cellular viability but not significantly. Potential reasons why the control room filter samples reduced cellular viability may be explained later in the metabolomics data.

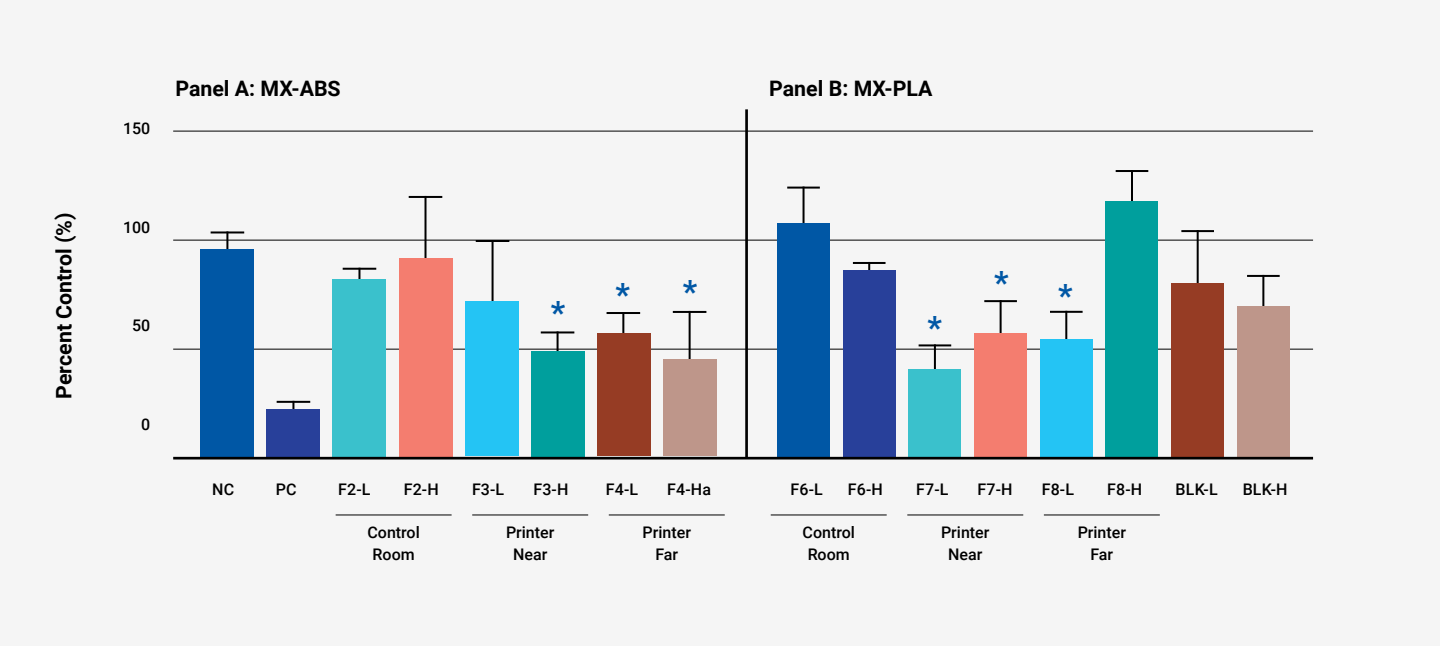

Figure 1: Cellular Viability of Primary Small Airway Epithelial Cells (SAEC) Exposed to ABS and PLA 3DP Particle Emissions Collected at the High School.

However, in sum, ABS appears to have higher toxicity as the particles collected farther from the printer induced greater reductions in cellular viability than PLA when comparing the high doses only. This suggests that proximity to 3DP during printing should be discussed when recommending safety guidelines along with ventilation and filtration mitigation strategies.

Figure 2 shows the cellular viability of SAEC after 24 hour exposure to 3DP emissions collected within a biosafety cabinet located within the university science center. In **Panel A**, we show a significant reduction (32.4%) in high doses of 3DP ABS emission (F1-H) collected near the printer. Likewise, low (F5-L) and high (F5-H) doses of 3DP ABS emission collected far from the printer location were found to reduce the cellular viability by 34.7% and 30.9%, respectively. A separate study investigating the 3DP emissions outside of the biosafety cabinet (OBS) was also conducted. In these OBS studies, F10-L and F10-H 3DP emissions showed slight but insignificant reductions (19% and 18%) in cellular viability. Within the lab space where these emissions were generated and collected, it was noted that the ventilation or airflow was higher, which may have contributed to dilution of the particle and chemical of the ABS emissions thus potentially lowering the toxicity of these particular emissions.

Panel B illustrates SAEC cellular viability after 24 hour exposure to emissions collected during a 3 hour PLA printing process. Neither sample at the low or high doses, (F12-L,F12-H) nor (F15-L,F15-H), which were collected near the printer during the 3 hour print diminished cellular viability of SAEC. Given the differences in levels of cellular viability reduction for both ABS and PLA emissions, this data suggests that the site conditions of the university are different from the site conditions at the high school. Specifically, when comparing PLA emissions collected at the high school compared to those collected at the university, the near low doses (F7-L and F15-L) were significantly different (p-value=0.0432), meaning that emissions from 3 hour printing of PLA at the high school were more toxic than a 3 hour PLA print performed at the university.

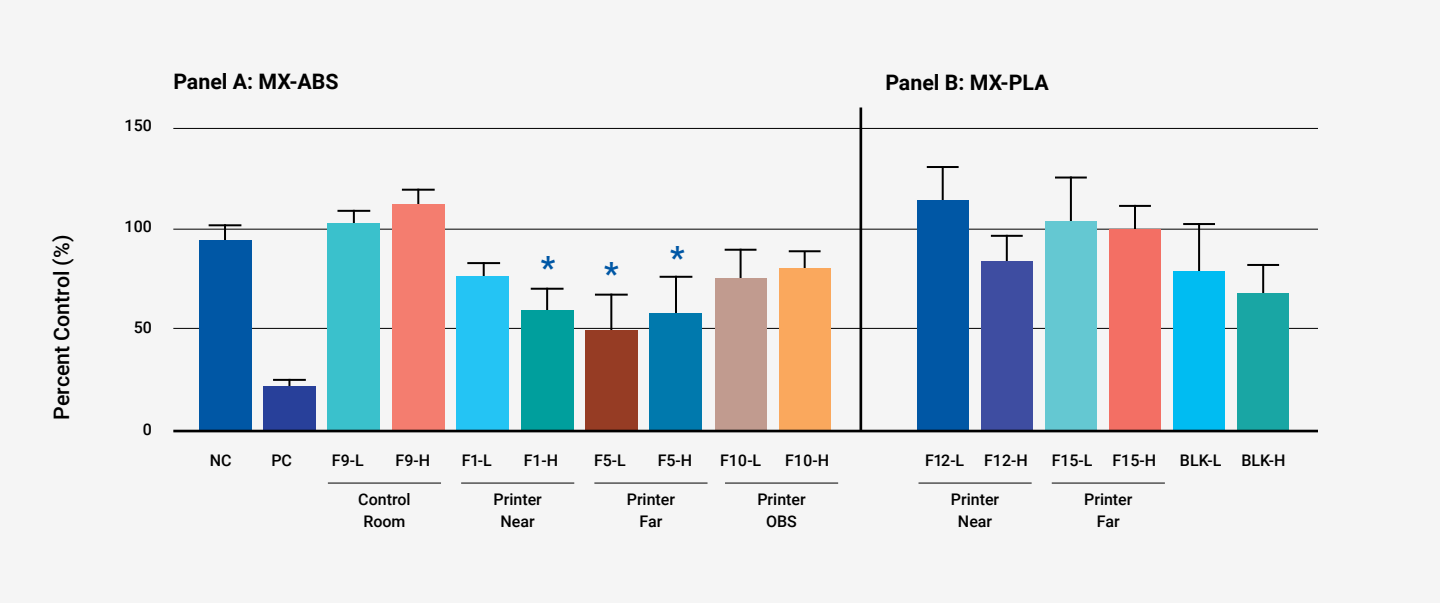

Figure 2: Cellular Viability of SAEC Exposed 3DP Emissions Collected at the University.

4.3 GENOTOXICITY OF ABS AND PLA EMISSIONS COLLECTED AT THE HIGH SCHOOL AND UNIVERSITY

After 24 hour exposure to 3DP emissions collected at the high school in July, the gamma-H2AX ELISA assay was performed. This assay determines the levels of gamma-H2AX, which is a biomarker of double DNA strand breakage found within cellular lysates. When DNA damage occurs in the form of double stranded breaks, the histone or protein that DNA is supported by becomes phosphorylated. Upon phosphorylation, gamma-H2AX is formed, which is the first step in recruiting and localizing DNA repair proteins. Thus, the detection of gamma-H2AX is a sensitive biomarker of chemical and environmental genotoxins (Kuo et al.).

In **Figure 3**, the y-axis is represented by the relative luminescence units or RLUs, while the x-axis consists of the printer location and exposure groups. A significant increase in gamma-H2AX can be observed due to the high dose of F3, which are samples collected near the printer during a 3 hour print of ABS. Likewise, the high dose of PLA collected from a far distance away from the 3DP (F8-H) also caused an increase in gamma-H2AX. Interestingly, the control room filter samples also caused a significant increase in gamma-H2AX, which may suggest other contaminants may exist within high school classrooms.

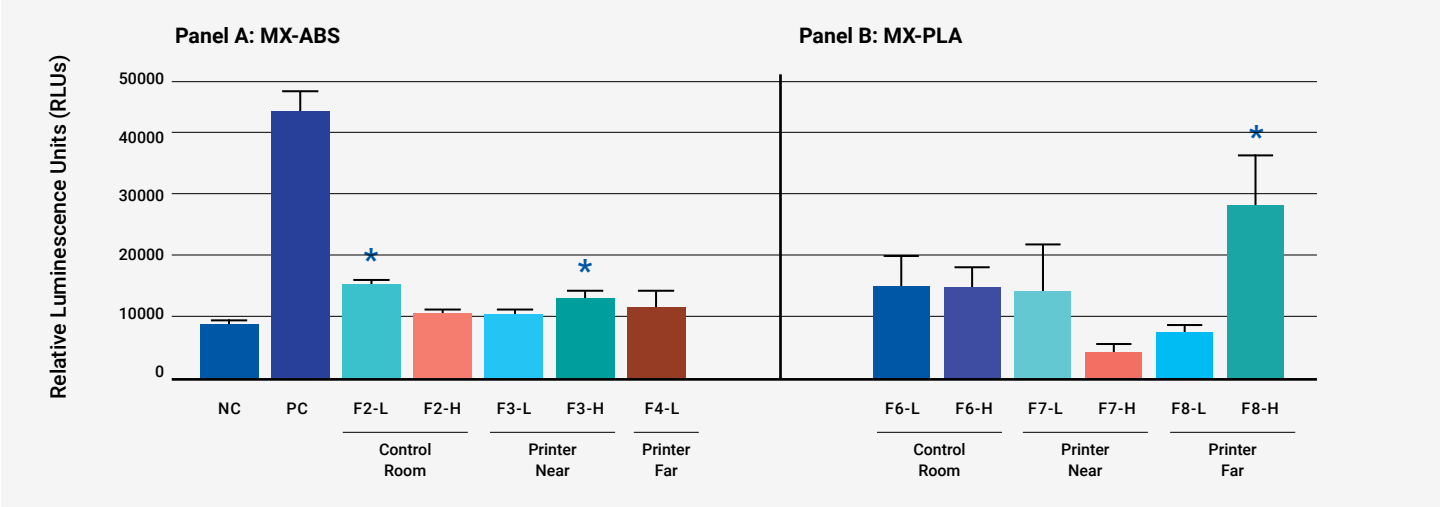

Figure 3: Gamma-H2AX Levels Caused by 3DP Emissions Sampled from the High School in July.

Figure 4 displays the gamma-H2AX levels elicited by 3DP emissions collected at the university. In comparison to the negative or untreated control cells and the low dose control room (F9-L), ABS emissions collected near the printer were significantly more genotoxic than those sampled further away from the printing process **(Figure 4 Panel A)**. Interestingly, emissions obtained near the printer but OBS at the low dose (F10-L) caused significant levels of double stranded breaks and hence an elevation of the gamma-H2AX biomarker. In **Figure 4 Panel B**, we show a prominent increase in gamma-H2AX biomarker from both high (F12-H) and low doses (F12-L) of emissions collected near the PLA printing process in a separate biolab space used for microbiology research. Conversely, PLA emissions collected within the conference room of the university campus did not increase the gamma-H2AX biomarker after 24 hours. This data also highlights the importance of accurately characterizing the site location. Notably, 3DP emissions collected from various locations within sites contributed to higher levels of DNA damage in the form of gamma-H2AX, a prominent biomarker of double stranded DNA breaks.

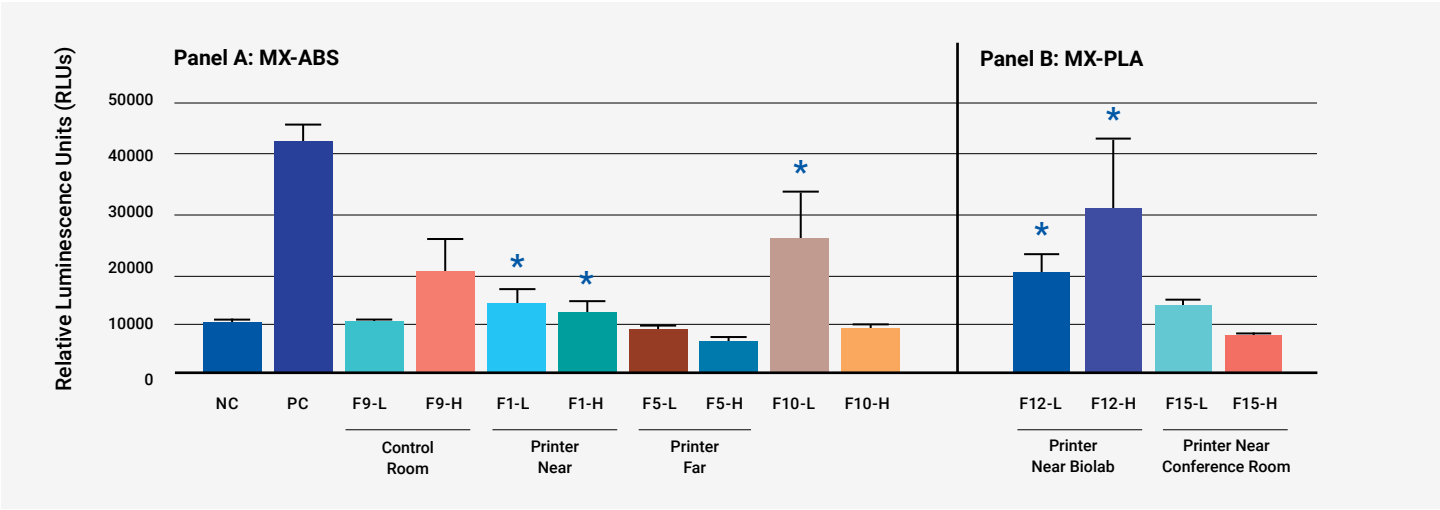

Figure 4: Gamma-H2AX levels Elicited by 3DP Emissions Collected at University Sites/Locations.

4.4 ABS AND PLA FILAMENTS ELICIT UNIQUE METABOLOMIC FINGERPRINTS RELATED TO CELLULAR INJURY, INFLAMMATION AND OXIDATIVE STRESS

Metabolomic profiling is the quantification of low-molecular weight metabolites and their intermediates that indicates the dynamic response to genetic modification and/or pathophysiological stimulation (Clarke et al., 2008). Hence, metabolomic profiling is a novel tool into understanding mechanisms of toxicity and associated outcomes.

Supernatants obtained from exposures to the high school and university 3DP filter samples were submitted to Purdue University for metabolomic profiling analysis. In **Table 3**, the metabolites altered due to the high school filter samples during a 24 hour exposure duration are displayed. ABS 3DP emissions increased 176 metabolites and decreased 214 for a total of 390 altered metabolites. In comparison to the high school control room, filter samples collected during a three hour PLA printing process were found to cause a higher alteration in total metabolites (n=404 vs n=347). Within these alterations, 157 metabolites were increased and 247 were decreased due to PLA 3DP emissions. In **Venn Diagram A**, the metabolites for the control room and ABS are shown, where 241 shared metabolites were observed and 149 unique metabolites due to ABS emission exposures were found.

In comparison, 106 unique metabolites for the control room were detected. In **Venn Diagram B**, unique and shared metabolites are provided. After 24 hour exposures, 209 shared metabolites were observed due to PLA 3DP and the high school control room emissions collected over a three hour printing or sampling period. Unique metabolites for the control room were 138 and 195 caused by PLA 3DP 24 hour exposures. **Venn Diagram C** illustrates the unique metabolites that ABS (n=133) or PLA (n=147) elicited during the 24 hour exposure along with the shared metabolites (n=257).

Table 3: Alteration of metabolites in saec exposed to high school (HS) filter samples after 24hr

Exposure Group	Total Metabolites Altered (p<0.05)	Increased	Decreased
HS Control	347	192	155
HS ABS	390	176	214
HS PLA	404	157	247

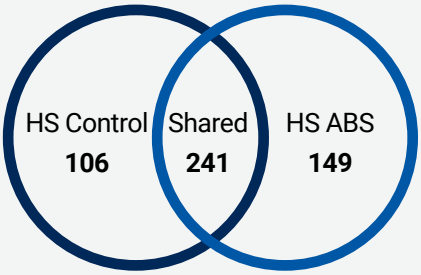

Venn Diagram A: Unique and shared metabolites generated by high school (HS) control room and ABS exposures.

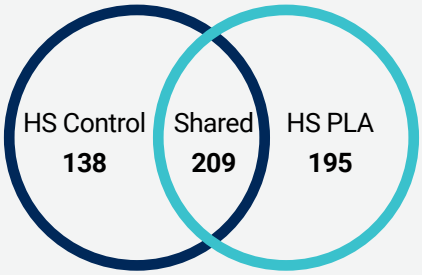

Venn Diagram B: Control room and PLA metabolites that are shared and uniquely expressed by each exposure group are highlighted.

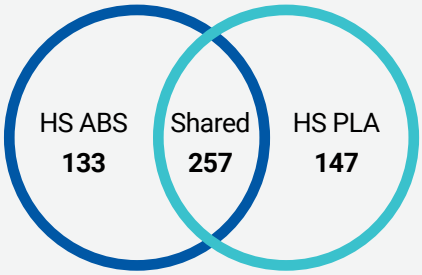

Venn Diagram C: Comparison of unique and shared metabolites elicited by high school (HS) ABS and PLA exposures.

In **Table 4**, metabolites that altered significantly due to extracted filter samples obtained from the university are displayed. Within the significantly altered metabolites, a total of 514 were due to the samples obtained from the university control room, where 241 were increased and 273 were decreased. Conversely, 301 metabolites were significantly altered due to 24 hour exposures of ABS 3DP emission, where 153 were increased and 148 were decreased.

Table 4: Alteration of metabolites in saec exposed to university filter samples after 24hr

Exposure Group	Total Metabolites Altered (p<0.05)	Increased	Decreased
UNI Control	514	241	273
UNI ABS	301	153	148

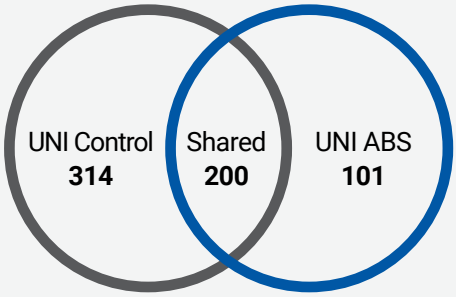

Venn Diagram: Shared and unique metabolites induced by each exposure group.

Of the total 514 metabolites elicited by the university control room, 314 were found to be unique in comparison to the ABS emissions collected in a nearby room as displayed in the associated **Venn Diagram**. There were 200 shared metabolites between the two exposure groups. Conversely, 101 unique metabolites were found in supernatants of SAEC exposed to ABS 3DP collected emissions.

While we were successful in identifying hundreds of metabolites, several metabolites were unable to be identified within the current databases utilized. However, of the several hundred that were identifiable through PubChem and produced a fold change of two or more, the vast majority of metabolites were associated with oxidative stress, cellular injury, and inflammation. For example, prostaglandins are synthesized through the metabolism of arachidonic acid via the cyclooxygenase pathway. When the body is functioning normally, baseline levels of prostaglandins are produced by the action of cyclooxygenase-1. When the body is injured (or inflammation occurs in any area of the body), cyclooxygenase-2 is activated and produces extra prostaglandins, which help the body to respond to the injury. Prostaglandin F2α (PGF2α), acting through the FP receptor, causes smooth muscle contraction and exhibits potent inflammatory activity. Both 17-phenyl trinor PGF2α and 16-phenoxy tetranor PGF2α are metabolically stable analogs of PGF2α and therefore biomarkers of both inflammation and cellular injury.

In **Figure 5**, we show fold-changes in 17-phenyl trinor PGF2α ethyl amide and 16-phenoxy tetranor PGF2α methyl amide due to 3DP emissions of both PLA and ABS. In **Figure 5 Panel A**, 3DP emissions of ABS collected at the high school caused a significant fold change in levels of 17-phenyl trinor PGF2α ethyl amide in comparison to emissions obtained from high school control room. Likewise, ABS emissions obtained from the university also elicited a substantial increase in 17-phenyl trinor PGF2α ethyl amide **(Figure 5 Panel B)**. Levels of 16-phenoxy tetranor PGF2α methyl amide were also significantly enhanced after 24 hour exposures to ABS 3DP emissions collected at the high school **(Figure 5 Panal C)**. Similarly, a significant increase in this potent inflammatory mediator was also observed due to ABS emissions obtained from the university **(Figure 5 Panel D)**.

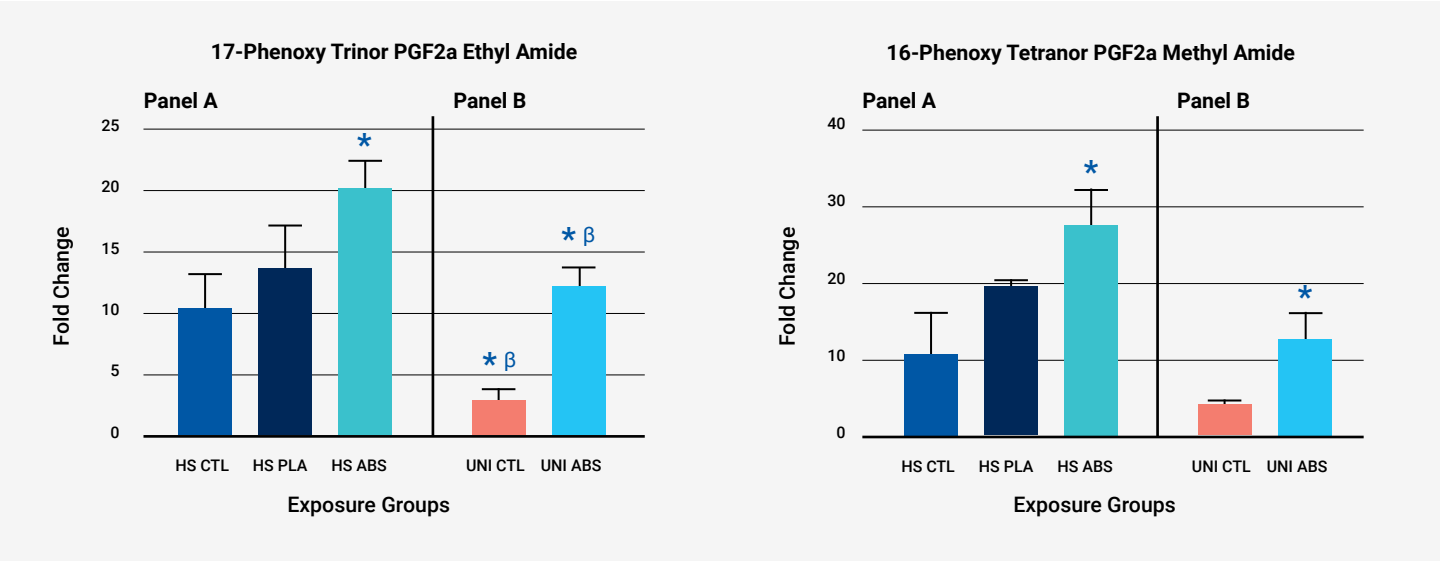

Figure 5: Alterations in Prostaglandins Induced by 3DP Emissions Collected at the High School and University. Beta (β) indicates significance between HS ABS and UNI ABS fold change levels.

In **Figure 6 Panal A**, 3DP emissions of ABS induced a significant elevation of prostaglandin E2 in comparison to samples collected in the control room at the high school. Similarly, ABS emissions collected during a three hour print at the university also caused a significant elevation in prostaglandin E2 **(Figure 6 Panel B)**.

As one of the most abundant prostaglandins in the body, prostaglandin E2 is involved in almost all typical inflammation markers and plays an important role in pathogenesis of immune disorders (Kawahara et al., 2015). An imbalance in production, breakdown, or both between prostaglandin E2 and other prostanoids possibly due to epithelial damage may be involved in the pathogenesis of moderate-to-severe asthma. Thus, prostaglandin E2 is a potent mediator of inflammation and immunity pathways. Specifically, prostaglandin E2 exerts diverse effects on cell proliferation, apoptosis, angiogenesis, inflammation and immune surveillance (Nakanishi et al., 2013). Interestingly, prostaglandin E2 can also have anti-inflammatory effects that are both potent and context dependent. Thus, accumulating data suggest that prostaglandins not only contribute to initiation of inflammatory processes but may also act in the resolution of inflammation (Scher et al., 2009).

Alongside the prostaglandins noted above, the metabolomic analysis revealed alterations in byproducts resulting from oxidative stress. Within the lung, pulmonary surfactants play a critical role in protecting the epithelial cell lining of the airways, thus maintaining the physical barrier between the lungs and inhaled pollutants. However, when high levels of oxidants are inhaled, the surfactant phospholipids may become oxidized resulting in oxidized phospholipids such as glycerophosphocholine and phosphatidylcholine.

In regard to glycerophosphocholine, studies have linked elevations in this oxidized phospholipid to lung injury caused by cigarette smoking (Kimura et al., 2012). Conversely, declines in phosphatidylcholine have been associated with acute respiratory distress syndrome (Simonato et al., 2011) and acute lung injury (Zhen et al., 1997).

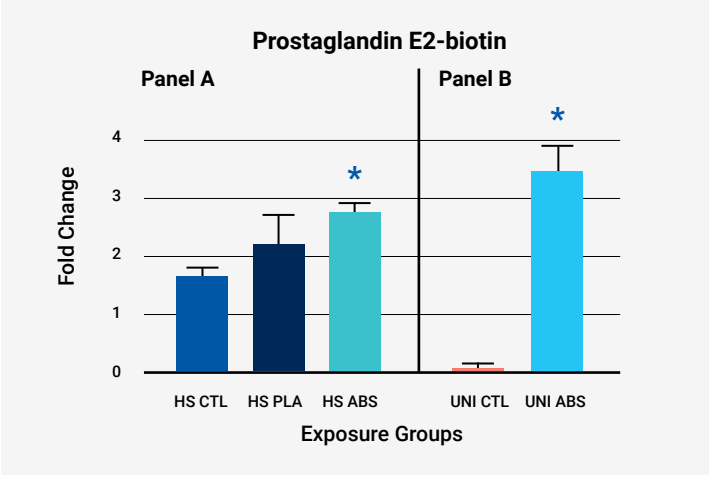

Figure 6: Modulation of Prostaglandin E2, a Potent Mediator of Inflammation and Immunity Pathways, by 3DP Emissions Obtained at the High School and University.

In **Figure 7A**, we show a significant elevation in glycerophosphocholine due to both ABS and PLA 3DP emissions collected at the high school, which indicates oxidative stress. ABS emissions collected at the university also caused a marked increase in glycerophosphocholine. In contrast, we observed higher levels of phosphatidylcholine caused by PLA 3DP obtained from the high school in comparison to the control room filter samples. On the other hand, we show a decline in phosphatidylcholine due to ABS 3DP high school samples in comparison to PLA 3DP emissions, which indicates cellular injury and oxidative stress.

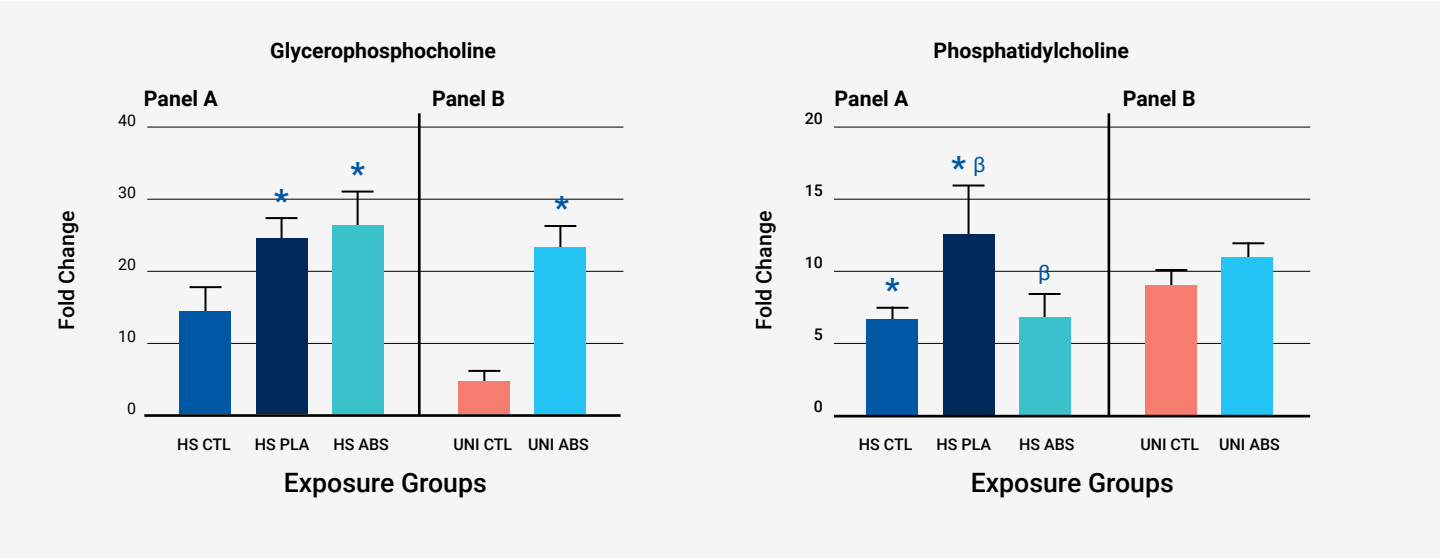

Figure 7: Alterations in Surfactant Phospholipids Including A) Glycerophosphocholine and B) Phosphatidylcholine Indicating Oxidative Stress Due to 3DP.

5.0 Conclusions

The data presented herein indicate ABS filament emissions may be more biologically active than PLA. Although contaminants were found at the high school site, ABS filament emissions and associated exposures contributed to a significant decline in small airway epithelial viability, oxidative stress, an increase in double stranded DNA breaks, and high levels of metabolites associated with cellular injury and inflammation. The metabolomics analysis from the university also suggest that ABS is more biologically active where significant elevations in 17-phenyl trinor PGF2α ethyl amide, 16-phenoxy tetranor PGF2α methyl amid, and prostaglandin E2 were found due to ABS 3DP emissions/exposures. Further, oxidative stress byproducts also indicate higher biological activity due to ABS 3DP exposures. Interestingly, although PLA 3DP samples collected at the university did not contribute to overt cellular toxicity in small airway epithelial cells, we did observe an increase in gamma-H2AX – a well-known biomarker of double stranded DNA damage. These data suggest that 3DP emissions, even at low levels, may contribute to cellular injury, inflammation, and oxidative damage of important biomolecules including DNA and phospholipids.

References

1. Kuo LJ, Yang LX. Gamma-H2AX - a novel biomarker for DNA double-strand breaks. In Vivo. 2008 May-Jun; 22(3):305-9. PMID: 18610740.
2. Clarke CJ, Haselden JN. Metabolic Profiling as a Tool for Understanding Mechanisms of Toxicity. *Toxicologic Pathology*. 2008;36(1):140-147. doi:10.1177/0192623307310947
3. Peebles RS Jr. Prostaglandins in asthma and allergic diseases. Pharmacol Ther. 2019 Jan;193:1-19. doi: 10.1016/j.pharmthera.2018.08.001. Epub 2018 Aug 3. PMID: 30081047; PMCID: PMC6309751.
4. Takemura M, Niimi A, Matsumoto H, Ueda T, Yamaguchi M, Matsuoka H, Jinnai M, Chung KF, Mishima M. Imbalance of endogenous prostanoids in moderate-to-severe asthma. Allergol Int. 2017 Jan;66(1):83-88. doi: 10.1016/j.alit.2016.05.013. Epub 2016 Jul 12. PMID: 27424536.
5. Kawahara K, Hohjoh H, Inazumi T, Tsuchiya S, Sugimoto Y. Prostaglandin E2-induced inflammation: Relevance of prostaglandin E receptors. Biochim Biophys Acta. 2015 Apr;1851(4):414-21. doi: 10.1016/j.bbalip.2014.07.008. Epub 2014 Jul 17. PMID: 25038274.
6. Nakanishi, M., & Rosenberg, D. W. (2013). Multifaceted roles of PGE2 in inflammation and cancer. Seminars in immunopathology, 35(2), 123–137. https://doi.org/10.1007/s00281-012-0342-8
7. Scher JU, Pillinger MH. The anti-inflammatory effects of prostaglandins. J Investig Med. 2009 Aug;57(6):703-8. doi: 10.2310/JIM.0b013e31819aaa76. PMID: 19240648.
8. Kimura T, Shibata Y, Yamauchi K, Igarashi A, Inoue S, Abe S, Fujita K, Uosaki Y, Kubota I. Oxidized phospholipid, 1-palmitoyl-2-(9'-oxo-nonanoyl)-glycerophosphocholine (PON-GPC), produced in the lung due to cigarette smoking, impairs immune function in macrophages. Lung. 2012 Apr;190(2):169-82. doi: 10.1007/s00408-011-9331-2. Ep
9. Simonato M, Baritussio A, Ori C, Vedovelli L, Rossi S, Dalla Massara L, Rizzi S, Carnielli VP, Cogo PE. Disaturated-phosphatidylcholine and surfactant protein-B turnover in human acute lung injury and in control patients. Respir Res. 2011 Mar 24;12(1):36. doi: 10.1186/1465-9921-12-36. PMID: 21429235; PMCID: PMC3072954.
10. Zhen, S., Li, H. & Sun, B. Decrease of disaturated phosphatidylcholine in acute lung injury in adult rats with ischemia-reperfusion of intestine † 1630. Pediatr Res 41, 274 (1997). https://doi.org/10.1203/00006450-199704001-01649